Titre: Title:	Convective response of a mass of water to a constant cooling rate applied on its boundaries
Auteurs: Authors:	Luc Robillard, & Patrick Vasseur
Date:	1981
Type:	Rapport / Report
Référence: Citation:	Robillard, L., & Vasseur, P. (1981). Convective response of a mass of water to a constant cooling rate applied on its boundaries. (Technical Report n° EP-R-81-21). https://publications.polymtl.ca/6230/

SERVICES DE LA RECHERCHE

Rapport Technique EP81-R-21
Classification: Library of Congress No.....

CONVECTIVE RESPONSE OF A MASS OF WATER TO A CONSTANT COOLING RATE APPLIED ON ITS BOUNDARIES

by

L. Robillard and P. Vasseur

May 1981

Ecole Polytechnique de Montréal

Campus de l'Université
de Montréal
Case postale 6079
Succursale 'A'
Montréal, Québec
H3C 3A7

CONVECTIVE RESPONSE OF A MASS OF WATER TO A CONSTANT COOLING RATE APPLIED ON ITS BOUNDARIES

by

L. ROBILLARD and P. VASSEUR

Ecole Polytechnique, Université de Montréal
Department of Civil Engineering
Montréal, P.Q., Canada

CONVECTIVE RESPONSE OF A MASS OF WATER TO A CONSTANT COOLING RATE APPLIED ON ITS BOUNDARIES

BY

L. ROBILLARD AND P. VASSEUR

Ecole Polytechnique, Université de Montréal
Department of Civil Engineering
Montreal, P.Q., Canada

ABSTRACT

The transient natural convection of a mass of water contained in a closed cavity with wall temperature decreasing at a steady rate is considered. For situations where a linear density temperature relationship can be assumed, a quasi steady state following an initial transient may be reached provided that the cooling rate applied to the wall is held constant long enough. Steady state flow characteristics in the case of a specific geometry are function of a single parameter, the Rayleigh number, in which a dimensionless temperature, based on the cooling rate, is used. For the particular case of water cooled through 4°C, temperature at which a maximum density occurs, a linear variation of density with respect to temperature is no more acceptable. However, it can be assumed that a linear relationship between the water thermal expansion coefficient and the temperature is valid in the neighbourhood of 4°C. With such an assumption it is still possible to characterize the cooling process that follows the initial transient by a single parameter. Detailed numerical results are presented for the particular case of a square cavity. Existing experimental and numerical results for the case of a horizontal circular pipe are also discussed.

1. INTRODUCTION

Natural convection flows in cold water are strongly affected by the occurrence of a density extremum with temperature variation. Thus at a temperature T = 3.98°C, the density of water attains a maximum value, thereafter decreasing in a non linear manner as the temperature passes this critical value. It results from this peculiar behaviour that the usual linear approximation of the temperature effect on density, used in conventional analysis, must be replaced by another more realistic density equation of state. This latter must be capable to approximate with precision not only the presence of the density extremum at 3.98°C but also the nonlinearity of the density dependence in the neighbourhood of this point.

The first studies demonstrating reversals of convective motion around the density extremum were reported almost simultaneously by Codegone (1939) and Powel (1940). The earliest theoretical study on the effect of density extremum on natural convection is due to Merk (1954) who predicted a minimum Nusselt number for melting spheres at 5.31°C. A brief experimental report by Dumore et al. (1953) together with some results from a vertical nonmelting plate by Ede (1951) generally supported Merk's analysis. Since these pioneering works, the problem of buoyancy-induced flows in cold water have been studied by many investigators not only because of their intriguing features but also due to the fact that they are a very commun occurrence in our environment and in many processes in technology.

Recent litterature on the effects of maximum density on natural convection may be classified in three different kinds of motion, namely external flow caused by a localized heat source; circulation,

which may occur in horizontal and unstably stratified fluid layers; and flows inside cavities. In the present study we consider only natural convection in enclosures. However, the current litterature will be now reviewed for the three types of motions, for reference purpose.

External flows in cold water have been throughly investigated in the past for flat, spherical and cylindrical surfaces. For instance, heat transfer rates, temperature profiles, and velocity gradientsproduced by a heated vertical plate in water in the region of 3.98°C were determined experimentally and theoretically by Schechter and Isbin (1958) and Vanier & Tien (1967, 1968). An exhaustive investigation of the convection flows adjacent to a vertical isothermal surface in cold or saline water has been presented recently by Carey, Gebhart & Mollendorf (1980). Temperature conditions for which local buoyancy force reversals occurs across the thermal boundary layer have been determined analytically. Surface heat transfer rate for flows with large buoyancy-force reversal was found to be only 50% of that for flows with no buoyancy-force reversal. Merk (1954) showed that third-order density polynomials for water could be successfully utilized in the boundary layer equations. Measurements by Oborin (1967) and Schenk and Schenkels (1968) for spheres in cold water are in fair agreement with Merk's prediction of convective inversion. However, as demonstrated by Carey et al (1980), an integral boundary layer treatment for such flow may be quite unrealistic. Using photographic techniques, Tkachev (1953) found a minimum Nusselt number of melting ice cylinder at 5.5°C. Tkachev was apparently the first worker to suggest that under certain conditions the flow within the boundary layer might be dual (i.e. up and down). More recently the natural convection over a horizontal ice cylinder has

been studied numerically by Saitoh & Hirose (1980). It was found that three-dimensional flow instability is induced in the vicinity of the minimum heat transfer region. The water temperature over which such instability occurs ranged from approximately 5.5°C to 6.5°C.

Circulations in horizontal fluid layers of cold water have been considerably studied because of their importance in several areas of geophysical fluid. The influence of the density anomaly on the onset of convection of such layers of fluid has been investigated by Veronis (1963) and Merker et al (1979), using the linear stability theory. Results are presented in terms of critical Rayleigh numbers and stability diagrams. Yen et al (1969) observed a regular cell structure in a melting ice layer heated from below. Numerical and experimental studies with a melting ice layer heated from above have been carried out by Seki et al (1977). In all those studies it was found that the density inversion plays an influential role on the onset of free convection and the free convection heat transfer. Concerning the convection process in cold water layers, no analytical solution is available due to the complex governing equations, the stability problem involved and the density anomaly of water.

The behaviour of convective motion of enclosed water, in the region of maximum density, has been studied for several different geometries, boundary conditions and temperature gradients. Desai and Forbes (1975) and Watson (1972) have studied numerically the heat transfer and flow patterns in cold water in a rectangular enclosure with vertical boundaries maintained at different temperatures and insulated horizontal boundaries. The flow was bicellular, in contrast to the one cell flow obtained for a fluid without maximum density effect and the

heat transfer occurred primarily by conduction. The transient behaviour of water, contained in rigid rectangular insulator and cooled from above to near freezing has been considered by Forbes & Cooper (1975). Vasseur and Robillard (1980) have studied the transient cooling of water, enclosed in a rectangular cavity with wall temperature maintained at 0°C. Supercooling of water contained in an enclosure subjected to convection boundary condition has been investigated by Cheng et al. (1978) for the case of a circular pipe and Robillard & Vasseur (1980) for a rectangular cavity. It was found that the resulting flow motion is greatly influenced by the presence of a maximum density effect. This latter slows down the initial circulation inside the cavity and subsequently reverses it. The resulting heat transfer is thus reduced in comparison to a standard situation without maximum density effect.

The present study considers the transient recirculating flow of cold water induced in a closed cavity by decreasing the wall temperature at a constant time rate. Cooling of the cavity is maintained long enough for the water temperature to encompass the 3.98°C point. Theoretical analysis on transient natural convection in enclosures with a uniform fluid temperature and a linear variation of wall temperature with time has received little attention in the litterature. Prior studies on the subject have examined theoretically (Quack (1970), Takeuchi & Cheng (1976)) and experimentally (Deaver & Ecker (1970)) the transient natural convection in horizontal cylinders with constant cooling rate for temperature conditions such that there is no maximum density effect. It was found that after an initial transient period, a quasi-steady state takes place inside the cavity and the developement of a correlation equation for Nusselt number is possible. An experimental investi-

gation on the cooling of water in a horizontal cylinder through the maximum density point has been presented by Gilpin (1975). Four flow regimes were identified, namely transient, quasi-steady, inversion and quasi-steady states before the occurrence of the freezing process. These findings are in agreement will Gilpin's quasi-steady state boundary layer model and a numerical study conducted by Cheng and Takeuchi (1976). Numerical results were obtained for three cases involving different cooling rates, pipe diameters and initial water temperatures. The importance of the inversion process, due to the maximum density effect, on the flow pattern preceeding the formation of ice inside the water pipe was evidenced by these authors.

In this paper, the convection of a mass of water with boundaries cooled at a constant rate is considered through a dimensional analysis based on the assumption of a linear relationship between the thermal expansion coefficient and the temperature. Exhaustive results for the specific case of a square cavity are obtained by a standard numerical method and conclusions of general character are withdrawn. The particular thermal boundary conditions of the present problem, when applied to a rectangular cavity introduce density gradients at the four boundaries. On one hand, driving forces are generated near the vertical walls in a way comparable to more standard situations where the two vertical walls are maintained at different temperatures (e.g. Patterson and Imberger, 1980). On the other hand an unstable layer is formed and one of the two horizontal walls, as it occurs when a cavity is heated from below (Linthorst et al. 1980).

2. PROBLEM FORMULATION

Consider the natural convective motion of a mass of water contained in the closed rectangular two-dimensional cavity illustrated schematically in figure 1. The aspect ratio of the half cavity is denoted by $E = h/b$. A rectangular Cartesian co-ordinate system is located in the centre of the base. Initially the water is motionless and at a uniform temperature T_i higher than 3.98°C. At time $t = 0$ a uniform temperature $T_w = T_i - ct$, where c is a constant cooling rate, is imposed on the boundaries of the cavity. Cooling of the system is maintained long enough so that the water maximum temperature inside the cavity reaches a value below 3.98°C.

The appropriate equations governing the resulting transient flow of fluid in this situation are:

$$\frac{\partial u'}{\partial t'} + u' \frac{\partial u'}{\partial x'} + v' \frac{\partial u'}{\partial y'} = - \frac{1}{\rho_m} \frac{\partial p'}{\partial x'} + \frac{\rho - \rho_m}{\rho_m} g + \nu \nabla^2 u' \qquad (1)$$

$$\frac{\partial v'}{\partial t'} + u' \frac{\partial v'}{\partial x'} + v' \frac{\partial v'}{\partial y'} = - \frac{1}{\rho_m} \frac{\partial p'}{\partial y'} + \nu \nabla^2 v' \qquad (2)$$

$$\frac{\partial T}{\partial t'} + u' \frac{\partial T}{\partial x'} + v' \frac{\partial T}{\partial y'} = \frac{k}{\rho_m C_p} \nabla^2 T \qquad (3)$$

$$\frac{\partial u'}{\partial x'} + \frac{\partial v'}{\partial y'} = 0 \qquad (4)$$

Here, u' and v' are vertical and horizontal velocity components, T the local temperature of fluid, P'the pressure, g the acceleration due to gravity and ρ, the density. ν, ρ_m, C_p, k and $\alpha=k/\rho_m C_p$ are the kinematic viscosity, density, heat capacity, thermal conductivity and thermal diffusivity, all refered to the temperature corresponding to the maximum density (3.98°C).

The initial and boundary conditions are:

$$
\begin{aligned}
&t' = 0 \quad u' = v' = 0 \; ; \quad T = T_i \text{ everywhere} \\
&t' > 0 \quad u' = v' = 0 \; ; \quad T_w = T_i - ct' \text{ on a solid boundaries} \qquad (5) \\
&\qquad \frac{\partial u'}{\partial y'} = v' = 0 \; ; \quad \frac{\partial T}{\partial y'} = 0 \text{ on the symmetry axis } (y' = 0)
\end{aligned}
$$

Inherent in the derivation of equations (1) and (2) is the usual Oberbeck-Boussinesq approximation (Chandraskhar 1961 and Gray & Giogini 1976). Also the works of compression and viscous dissipation are neglected and all fluid properties are assumed constant except for density in the buoyancy term (Booker 1976). Each of these assumptions introduces certain small inaccuracies, and the reference cited give discussions under which these inaccuracies become significant. For the present study none is of major importance.

The temperature dependent density for water in equation (1) is usually approximated in litterature by a polynomial which may take the form:

$$\frac{\rho - \rho_m}{\rho_m} = \sum_{j=1}^{n} \beta_j (T - 3.98)^j \qquad (6)$$

Vanier and Tien (1967) have already used a polynomial of comparable form. In the case of a fourth order polynomial, the numerical values of coefficients β_j may be deduced from Fujii (1974):

$$\begin{aligned} \beta_1 &= -.392313066 \times 10^{-7} \quad (^\circ C^{-1}) \\ \beta_2 &= .800323127 \times 10^{-5} \quad (^\circ C^{-2}) \\ \beta_3 &= -.825365644 \times 10^{-7} \quad (^\circ C^{-3}) \\ \beta_4 &= .873587655 \times 10^{-9} \quad (^\circ C^{-4}) \end{aligned} \tag{7}$$

With these coefficients in (6), it is possible to estimate the value of $(\rho - \rho_m)/\rho_m$ with great accuracy for the range 0-20°C.

It is seen from (6) and (7) that in the neighbourhood of 3.98°C the contribution is negligibly small for all terms except the second order term. In fact, according to Moore and Weiss (1973), a parabolic type relationship of the form

$$\frac{\rho - \rho_m}{\rho_m} = -\lambda(T - 3.98)^2 \tag{8}$$

with $\lambda = .8 \times 10^{-5}\ (^\circ C)^{-2}$ may be used within 4% over the range 0-8°C. The thermal expansion coefficient becomes:

$$\beta = -\frac{1}{\rho_m}\frac{\partial \rho}{\partial T} = 2\lambda(T - 3.98) \tag{9}$$

Defining the following dimensionless parameters:

$$x = \frac{x'}{b} \qquad y = \frac{y'}{b} \qquad u = \frac{u'b}{\alpha} \qquad v = \frac{v'b}{\alpha}$$

$$t = \frac{t'\alpha}{b^2} \qquad \theta = \frac{T - T_w}{\Delta T} \qquad \Delta T = \frac{cb^2}{\alpha} \tag{10}$$

introducing a dimensionless stream function ψ and a dimensionless vorticity ω such that

$$u = \frac{\partial \psi}{\partial y} \qquad v = -\frac{\partial \psi}{\partial x}$$

$$\omega = \frac{\partial v}{\partial x} - \frac{\partial u}{\partial y} \tag{11}$$

and using eqs (5), (8) and (9), one can reduce eqs (1) to (4) to the following nondimensional forms:

$$\frac{1}{Pr}\left(\frac{\partial \omega}{\partial t} + \frac{\partial u\omega}{\partial x} + \frac{\partial v\omega}{\partial y}\right) = Ra\,\frac{\partial \theta}{\partial y} + \frac{Ra'}{2}\,\frac{\partial \theta^2}{\partial y} + \nabla^2\omega \tag{12}$$

$$\nabla^2\psi = -\omega \tag{13}$$

$$\frac{\partial \theta}{\partial t} + \frac{\partial u\theta}{\partial x} + \frac{\partial v\theta}{\partial y} = \nabla^2\theta + 1 \tag{14}$$

with initial and boundary conditions:

$$\left.\begin{array}{lll} t = 0 & u = v = \omega = \psi = \theta = 0 & \text{everywhere} \\ t > 0 & u = v = \psi = \theta = 0 & \text{at } x = 0, E \text{ and } y = 1 \\ & \dfrac{\partial u}{\partial y} = v = \psi = \dfrac{\partial \theta}{\partial y} = \omega = 0 & \text{at } y = 0 \end{array}\right\} \tag{15}$$

There are no boundary conditions for the vorticity but indirectly:

$$\omega = - \frac{\partial^2 \psi}{\partial n^2} \quad \text{at } x = 0, E \text{ and at } y = 1 \tag{16}$$

n being a coordinate normal to the boundary.

For the specific case of a square cavity containing water, E = 2 and the Prandtl number Pr = ν/α is uniquely determined.

The unity (b^2 c $\Delta T/\alpha$ = 1) appearing on the right hand side of the energy equation (14) can be regarded as a uniform heat source term. As a matter of fact for situations where ρ is linearly related to T, the present problem is known to be equivalent to transient natural convection heat transfer between a fluid with uniform internal heat sources of strength per unit time and volume ρ c C_p and a cavity with constant wall temperature.

The parameter Ra appearing in (12) is a time dependent Rayleigh number defined as:

$$Ra = \frac{gb^3}{\alpha\nu} \beta_w \Delta T \tag{17}$$

in which β_w is the thermal expansion coefficient based on T_w, the temperature at the wall at a given time t. Since $\beta_w = \beta_i - 2\lambda\Delta Tt$ in the case of a parabolic relationship between ρ and T, equation (17) becomes:

$$Ra = Ra_i - Ra't \tag{18}$$

in which Ra_i is an initial Rayleigh number based on temperature T_i. Ra' is a parameter called non linear Rayleigh. It corresponds to the rate of decrease of Ra and is defined as:

$$Ra' = \frac{gb^3}{\alpha\nu} 2\lambda\Delta T^2 = -\frac{\partial Ra}{\partial t} \tag{19}$$

According to (12) non linearity effects between density and temperature are expected to be small at a given time t provided that the following condition:

$$\frac{Ra'\theta}{|Ra|} \ll 1 \quad \text{or} \quad \frac{T - T_w}{|T_w - 3.98|} \ll 1 \tag{20}$$

is satisfied.

In the numerical results, the dimensionless heat transfers across the top lateral and bottom boundaries and denoted by ϕ_T, ϕ_L and ϕ_B respectively are of interest. ϕ_T is defined as:

$$\phi_T = \frac{q_T b}{k\Delta T} = \int_0^1 \left(-\frac{\partial\theta}{\partial x}\right)_{x=\varepsilon} dy \tag{21}$$

in which q_T is the heat flux by unit area averaged over the top boundary. Similar expressions may be obtained for lateral and bottom boundaries. Furthermore it may be shown that the dimensionless heat transfer averaged over all boundaries corresponds to the following expression:

$$\phi_{av} = \frac{1}{2 + E}(\phi_T + \phi_B + E\phi_L) = \frac{E}{2 + E}\left(1 - \frac{\partial\bar{\theta}}{\partial t}\right) \tag{22}$$

in which $\bar{\theta}$ is the dimensionless temperature averaged over the cavity according to the following equation

$$\bar{\theta} = \frac{1}{E} \int_0^E \int_0^1 \theta \, dy \, dx \tag{23}$$

$\bar{\theta}$ is a measure of the heat energy in excess of the wall temperature contained in the cavity.

3. NUMERICAL APPROACH

In this study a two-dimensional alternating direction (A.D.I.) procedure is employed to solve the coupled transport and energy equations (12) and (14) which are quasi-linear, second-order partial differential equations of the parabolic type. The computational method involved differs slightly from that used by Mallison and de Vahl Davis (1973). The first and second derivatives are approximated by central differences and the time derivatives by a first order forward difference. The finite difference form of the equations are written in conservative form for the advective terms in order to preserve the transportive property (Roache 1976). The elliptic equation (13) for the stream function, is solved by the method of successive over-relaxation (S.O.R.) for the new field which is then used to obtain the velocities from (11) and the wall vorticity (which requires the velocity boundary conditions).

Boundary conditions on ψ and θ are applied in the usual manner, using central differences whenever possible and image points for derivative conditions. Exact boundary conditions for ω are not

known in the present problem. However, approximate values of ω on the boundaries can be obtained from the most recent estimates of either ψ or u and v, using (11). In the present study the second way is used since it was found, from numerical experimentations, that in general it yielded more stable results.

The determination of an appropriate mesh size is related to the complex questions of accuracy and stability. Patterson and Imberger (1980), in their numerical treatment of the square cavity use a time-length scale approach to estimate the limits of time-step and mesh size for accurate spatial and temporal representation of the solution. They conclude that maintaining two mesh points inside the boundary layer at each vertical level requires an excessive number of points when Ra reaches 10^6. For the present study, a maximum mesh size of 30 x 15 for the half cavity was found to be an acceptable compromise between the desired accuracy of the solution and the required computation time.

A check of the conservative properties of the algorithm was made at regular intervals during the computation by comparing the heat transfer ϕ_{av} to the rate of change of $\bar{\theta}$ according to equation (22). Simpson's rule was used for numerical integration and a three points finite difference approximation for $\partial\bar{\theta}/\partial t$.

In order to check the validity of the present numerical method, comparisons have been made with other existing solutions. An excellent agreement was observed, for low Rayleigh numbers, with the analytical Poot's solution (28). For higher Rayleigh numbers, the numerical results from Wilkes and Churchill (1968), for the case of heat transfer into a rectangular cavity, were integrally reproduced.

To expedite plotting of the results, an auxiliary computer program was written to locate points lying on specified isotherms and streamlines by linear interpolation of the computed values at the grid points. As mentioned earlier the problem under consideration is symmetrical and it was found advantageous to reproduce the computer results at a given time on a single graph with the flow pattern on the right half of the cavity and the isotherms on the left half.

4. RESULTS AND DISCUSSION

Equation (18) indicates that when Ra' is set equal to zero, the resulting Rayleigh number Ra caracterizing the present problem remains constant throughout the cooling process. This situation corresponds to the standard hypothesis of a linear relationship between density and temperature. However, if Ra' is given a finite value larger than zero, Ra decreases linearly with time. The resulting situation then corresponds to the cooling of a fluid having a non-linear relationship between its density and temperature, such as water at a temperature in the neighbourhood of 4°C . Both situations will be discussed in the following sections.

4.1 Results with Ra constant

The cooling with constant Ra of a mass of fluid contained in a horizontal circular pipe has been studied theoretically by Quack (1970) and Takeuchi and Cheng (1976) and experimentally by Deaver and Ecker (1970). It was found that, although the cooling process is a transient one, a quasi-steady state develops if the cooling rate is held constant long enough. This quasi steady state, as described by

Takeuchi and Cheng (1976) for the case of a circular fluid cylinder, is characterized by temperature differences between interior points and boundary which remain constant with time. Figure 2a gives $\bar{\theta}$, the dimensionless temperature averaged over the cavity, function of the cooling time t, for Ra = 5×10^4 and 3×10^5. The pure conduction case (Ra = 0) is reproduced for comparison purpose. For those three cases, at time t = 0, the fluid is motionless and at uniform temperature T_I. At the early stages of the cooling process, temperature gradients are set up near the walls. If motion is excluded, as it is the case for $|Ra| = 0$, a pure conduction quasi-steady state is reached for which $\bar{\theta} = .14$. If motion is allowed, temperature gradients introduce density differences. Near the side walls, those density differences generate driving forces; motion is set up and takes the form of two counter-rotating vortices with fluid moving downward near the side walls for Ra > 0. With time elapsing, a quasi steady state is reached for which $\bar{\theta}$ becomes independent of time and $\phi_{av} = .5$, according to equation (22), in the case of a square cavity. (E = 2). At quasi steady state, the value $(.14 - \bar{\theta})$ is a measure of the convective motion inside the cavity, this difference increasing with increasing Ra. Thus Ra represents a potential of convective motion, this latter being attained at steady state. The quasy steady state flow and temperature fields corresponding to Ra = 5×10^4 are represented in figure 2b on the right and left half of the cavity respectively, the symmetry condition prevailing throughout the computation. The specific configuration of the isotherms on the left half indicates that the top heat transfer ϕ_T is larger than the bottom heat transfer ϕ_B.

Figure 2c corresponds to Ra=3×10^5 and implies a relatively high convective motion for which a second mode of convection, consisting of

two additional rolls near the top boundary, is established inside the cavity. No comparable secondary motion has been reported by Takeuchi and Cheng (1970) for the case of the circular fluid cylinder. Secondary motions observed in the past were related either to the high aspect ratio of the cavity (Elder 1965) or to low Prandtl number effects (Charrier Mojtabi & al., 1979). In fact the second mode of convection observed in this study results essentially from the interaction between the zone of instability located near the top boundary and the flow field induced by the side wall. This situation arises from the particular geometry and thermal boundary conditions involved in the actual problem. Thus the origin of the secondary motion depicted in the present investigation seems more closely related to the multicellular flow arising from instabilities such as those obtained in the case of a cavity heated from below, for which a large variety of flow structures have been observed in the past, as discussed for instance by Linthorst and al. (1980). Therefore, some doubt arises about the appropriateness of a two dimensional approach to adequately describe the physical flow behaviour at large Ra. Nevertheless new modes of convection are expected to occur with increasing Ra and the present result provides a mean to investigate the behaviour of such flows when density extrema are present.

Quasi steady state results giving $\bar{\theta}$ as a function of Ra correspond to the heavy lines of figs 4a and 5a. Those lines may be obtained point by point, by solving numerically the basic equations with $Ra' = 0$ far enough in time to obtain the quasi steady state, the procedure being repeated for different Ra. Other steady state characteristics are given by heavy lines of figures 4b, c and 5b,c,d, θ_c being the

dimensionless temperature at the center of the cavity. The discontinuity observed on some of the heavy lines of figures 4 and 5, is located at Ra = $\pm$ 8 x 10^4 and separates the first and second mode of convection already mentioned.

Figure 4 shows results with Ra on arithmetic scale with negative range. The negative range corresponds to negative β_w in (17), i.e. to a situation for which density is decreasing with decreasing temperature, as it occurs for water below 3.98°C. The flow and temperature fields at negative Ra are the mirror image of those at corresponding positive Ra. $(\phi_T)_E$ behaves as $(\phi_B)_E$ and vice versa. Such a behaviour can be noticed on figures 4b and 4c. At Ra = 0, the heavy line $\bar{\theta}_E$ of figure 4a attains a maximum value of .14 with a sharp peak whereas $(\phi_T)_E$ and $(\phi_B)_E$ of figures 4c and 4d take the value .5 with maximum slope. Thus extrema for $\bar{\theta}$ and the derivatives of ϕ_T and ϕ_B are seen to occur at Ra = 0.

Logarithmic scale for Ra is used in figures 5 in order to cover the wide range involved in the numerical solution. Positive and negative range of Ra are superposed. As a consequence figure 5c shows two heavy lines with the top one corresponding to positive Ra and the bottom one to negative Ra. The converse is true for figure 5d.

4.2 Results with Ra decreasing linearly with time

When Ra decreases with time at a constant rate (Ra'), the initial transient is followed by a non linear transient, as illustrated in figure 3. In this figure, the time scale of figure 2 is replaced by a Rayleigh scale which corresponds also to a temperature scale with

3.98°C at Ra = 0. The three dashed lines are initial transients corresponding to cases with same Ra' = 2 x 10^5 but with different Ra_i , one of which (Ra_i = 1.47 x 10^5) having its flow and temperature fields reproduced on figure 6a. The three initial transients tend asymptotically to a single curve represented by a continuous line on figure 3. This curve is a non linear transient uniquely determined by the single parameter Ra'. Non linear transients exist for other physical quantities such as θ_c , heat transfers at boundaries or stream function. Once relieved of the initial transients, they form all together the essential features of the cooling through a maximum density.

It is possible to obtain the non linear transients to their full extent 1° by initiating the cooling process at a value Ra_i such that non linear effects are absent, inequality (20) being satisfied for all interior points and 2° by providing enough computer time to reach negative Ra such that (20) is again satisfied. Light lines of figures 4 and 5 represent non linear transients that have been obtained according to that approach. Among them are the non linear transients corresponding to Ra' = 2 x 10^5 of figures 3 and 6. On figures 5 these latter are represented by dotted lines. The direction of the cooling process is indicated by arrows on figures 5c and 5d. The heavy lines of figures 4 and 5 have already been described to be quasi steady states for cases where ρ varies linearly with T. Here they correspond to equilibrium states to which the fluid system tends, with a lag proportional to the rate of change of Ra. Non linear transients tend to join asymptotically equilibrium curves with Ra' θ/Ra becoming negligibly small. It is observed on figure 4, that when Ra has decreased sufficiently, $\bar{\theta}$, ϕ_T and ϕ_B will depart from the equilibrium curves $\bar{\theta}_E$, $(\phi_T)_E$ and $(\phi_B)_E$ respecti-

vely, this departure occurring earlier for higher Ra'.

4.3 The inversion process

It may be observed on figure 4a that the peak corresponding to a given Ra' shows a more or less pronounced lag with respect to Ra = 0, position along the abcisse where the peak of the equilibrium curve $\bar{\theta}_E$ is located. It is also observed that the peak value is smaller for larger Ra'. The pure conduction value of .14 for the equilibrium curve is due to the fact that, for Ra' $\to$ 0, there is no more convective heat transfer at Ra = 0. However, for finite Ra', convective motion is transported toward negative Ra and thus convective motion resulting from positive Ra is still present when negative Ra effects are acting to reverse the flow field. As a matter of fact, once Ra has become negative, temperature differences introduced near the boundaries start generating density gradients of opposite sign. An inversion process is thus initiated inside the cavity at the end of which the flow and temperature fields tend to become the mirror image of the ones at corresponding positive Ra. The higher is Ra', the more intense is the convective motion inside the cavity during the inversion process. This fact explains why the peak characterizing the non linear transient decreases with increasing Ra'. With progression of cooling process beyond the peak value for $\bar{\theta}$, i.e., with Ra becoming more negative, the density differences introduced near the boundaries become more pronounced. The new counter rotating motion set up inside the cavity is reinforced, and convective heat transfer is enhanced. As a consequence, $\bar{\theta}$ begins to decrease. Condition (20) is more and more satisfied and $\bar{\theta}$ tends asymptotically to the

equilibrium curve. Non linear transients are therefore connected to the equilibrium curve in both positive and negative directions and this observation is true for the other physical quantities such as θ_c and heat transfers at boundaries.

The sequence of events taking place during the inversion process may be observed on the set of figures 6a to 6f where flow and temperature fields corresponding to a moderate Ra' are illustrated. Figure 6a, with Ra = 1.4 x 10^5 corresponds to the initial transient described in section 4.2, during which temperature differences are being set up inside the cavity. The value of Ra_i involved in the present case (1.47x 10^5) is important enough for a second mode of convection to develop and, consequently, two pairs of conterrotating vortices are present inside the cavity (figure 6b) when the initial transient is over (see also figure 3). The initiation of the inversion process is depicted by figure 6c in which the occurrence of a small vortex of opposite rotation near the bottom corner indicates the beginning of the flow reversal. With time elapsing, this vortex grows and displaces the original one (figure 6d). Eventually a situation is reached where the original circulation is completely reversed, as shown on figure 6e. The new motion gradually brings the relatively warm fluid of the core region near the bottom boundary. With progression of the cooling process, the reversed convective motion is enhanced. A second mode of convection appears, with a pair of additional vortices near the bottom boundary, as shown on figure 6f. It is also noticed on this last figure that the temperature field, like the flow field, has become opposite in character to the one existing at positive Ra.

4.4 Transportive property of Ra' toward low temperatures

The extremum in density at 4°C gives rise to a very important change in flow behaviour within the laminar range of the cooling process. There are however other important changes such as the passage from one mode of convection to another along the Ra axis. As mentioned in section 4.1 the passage is abrupt in the case of the equilibrium curves with a finite jump separating first and second mode of convection at Ra = $\pm 8 \times 10^4$. For Ra' > 0, the passage from one mode to the other occurs later and is more gradual. For instance it may be observed on figure 4a that the jump occurring at Ra = -0.8×10^5 on the $\bar{\theta}_E$ curve is reported approximately at Ra = -1.3×10^5 and -1.8×10^5 on the non linear transients corresponding to Ra' = 2×10^5 and 5×10^5 respectively. Similar effects concerning the passage from one mode to the other are observed for the heat transfer curves of figures 4b and 4c. Thus, considering the lag created by Ra' on the flow reversal at 3.98°C and the lag also created by Ra' on the passage from one mode to the other it may be concluded that an important property of Ra' is to transport toward negative Ra the features of the convection which characterize the equilibrium state. Moreover, if Ra' is important enough, the second mode occurring at positive Ra will not disappear before the initiation of the inversion process at Ra=0 and will interact with it. The sequence of flow and temperature fields of figures 7a to 7f illustrates a case where Ra' is important enough for the secondary motion to be present when the inversion process starts. All figures of this sequence, including the first one, describe the non linear transient exclusively, no initial transient being involved. It can be noticed that figure 7f is almost the mirror image of figure 7a. Some flow characteristics can be readily

obtained for each of these figures from the corresponding non linear transients ($Ra' = 10^7$) of figures 5.

If very large values of $|Ra|$ are involved, the cooling process may start in the range of turbulent convection above 3.98°C and also end up in the turbulent range below 3.98°C. Here also it might be expected that turbulent features will be carried toward lower Ra thus reducing the laminar range. Large Ra' can be conceived for which turbulence is carried with enough strength to reach the inversion process and even to reach negative Ra where the reversed convection itself start generating turbulence. If the initial transient occurs in the turbulent range, a laminar range for the non linear transient will follow provided that Ra' is not too large, i.e., that enough time is given for viscous forces to absorb the turbulent motion of the system. The present numerical computation is, of course, limited to the laminar range. When large Ra values ($Ra \sim 10^7$) are involved, oscillations develop in the numerical results and parts of the curves corresponding to the occurrence of those oscillations are represented by dashed lines on figures 5.

4.5 Effects of the non linearity in the relationship between β and T

Each non linear transient of figures 4 and 5 describes adequately the behaviour of a mass of water cooled to a constant rate provided that temperatures involved remain in the neighbourhood of 3.98°C. Discrepancies will develop with increasing difference between T_w and 3.98°C. In fact, due to the non linearity between β and T, the rate of change of Ra, is slightly increasing with decreasing temperature, c being maintained constant. This tendency is more or less pronounced at a particular Ra, depending on $|T_w - 3.98|$. Strictly speaking, Ra'of (19)

corresponds to the exact rate of change of Ra only when $T_w = 3.98°C$. Figure 8 illustrates the kind of discrepancy to be expected. The heat transfer ϕ_{av}, given as a function of Ra is defined in (22) and is seen to vary according to the derivative of $\bar{\theta}$. The horizontal line at $\phi_{av} = .5$ is the equilibrium state $(\phi_{av})_E$, constant for any Ra. Two cases having the same Ra' are reproduced on figure 8. The computation of the two cases was done by using a fourth order polynomial in the relationship between ρ and T. Case 1, represented by a continuous line, covers a relatively narrow temperature range above and below 3.98°C, as indicated by its temperature scale. Case 2 is represented by a dashed line where it differs significantly from Case 1. Its temperature scale also given on figure 8 indicates that a wider range of temperature is covered. Discrepancies should appear at locations where high gradients occur. The first important gradient at $Ra \simeq -4 \times 10^4$ corresponds to the inversion process. The very slight discrepancies observed in the numerical results were not sufficient to produce distinct curves at this location. The second important gradient at $Ra \simeq -1.3 \times 10^5$ corresponds to the establishment of the second mode of convection following the inversion. Discrepancies produce distinct curves with the peak of Case 2 slightly at left. Corresponding temperature is $\sim -0.2°C$. Thus the parabolic approach in the present dimensional analysis appears to give fairly acceptable results provided that the temperature range at which the non linear transient differs from the equilibrium curve remains within the range 0 - 8°C.

4.6 Comparison with existing experimental data

In Gilpin's experiments (1975) on the cooling of a horizontal circular cylinder filled with water, the temperature at the center was recorded as a function of time for various diameters and cooling rates. Those experimental results, when transformed by the application of the present dimensional analysis, become the set of curves represented by the continuous lines of figure 9. It is observed that the trend of figure 5b is qualitalively reproduced. For the particular geometry involved here, the maximum possible value for θ_c, which corresponds to the pure conduction quasi steady state, is 0.25. Numerical results obtained by Cheng and Takeuchi (1976) for the same type of problem have also been transformed and reproduced on figure 9 (dashed lines). Those last curves are incomplete and not entirely relieved of the initial transients. Nevertheless their trend and ordering shows relatively good agreement with the previous ones.

CONCLUSIONS

The natural convection taking place in a mass of water near 3.98°C with boundaries subjected to a constant cooling rate has been investigated through a dimensional analysis based on a parabolic relationship between density and temperature. Although most graphics presented in this article concern specific numerical method and geometry (square cavity), general conclusions may be established with application to any geometry and to experimental as well as theoretical studies on the subject. In particular the following statements may be listed:

1° When density is linearly related to temperature, a quasi-steady state regime may be reached from initial conditions for which the fluid is at rest and at uniform temperature. The transient solution in characterized by a developing regime during which motion is set up inside the cavity. At sufficiently large time, velocities, flow patterns and temperature differences between the fluid and the wall become constant with time, indicating that the quasi steady state is reached;

2° The presence of a maximum density, as it is the case for water at 3.98°C, implies a decrease followed by a reversal and finally an increase of the convective motion inside the cavity;

3° When a maximum density is involved in the cooling process, non linear transients replace the quasi steady state results. Those non linear transients, relieved of the initial ones, are the essential features of the cooling process and are uniquely determined by a single parameter called the non linear Rayleigh number. The set of non linear transients obtained for different values of the non linear Rayleigh number forms an exhaustive solution for a given geometry.

4° Quasi steady state results obtained when the density is linearly related to the temperature correspond to equilibrium curves to which non linear transients tend asymptotically when the difference $|T - 3.98|$ is increased;

5° An important effect of the non linear Rayleigh number is to transport toward low temperatures the features of convection characterizing the equilibrium curves. A lag is so created between the non linear transient and the corresponding equilibrium curve, the importance of this lag being directly related to the value of the non linear Rayleigh number.

ACKNOWLEDGMENTS

This work was supported in part by the National Sciences and Engineering Research Council of Canada through grants A-4197 and A-9201 and jointly by the FCAC, Gouvernement du Québec, under grant number CRP 506-78.

REFERENCES

BOOKER, J.R. 1976 J. Fluid Mech. 76, 741.

CAREY, V.P., GEBHART, B. & MOLLENDORF, J.C. 1980 J. Fluid Mech. 97, 279.

CHANDRASEKHAR, S. 1961, Hydrodynamics and Hydromagnetic stability. Oxford University Press.

CHARRIER-MOJTABI, M.C., MOJTABI, A. & CALTAGIRONE, J.P. 1979 J. Heat Mass Transfer 101, 171.

CHENG, K.C. & TAKEUCHI, M. 1976 J. Heat Transfer, 581.

CHENG, K.C., TAKEUCHI, M. & GILPIN, R. 1978 Numerical Heat Transfer, 1, 101.

CODEGONE, C. 1939 Acc. Sci. Torino Atti 75, 1967.

DEAVER, F.K. & ECKERT, E.R.G. 1970 Heat Transfer, Vol. 4, Paper NC 1.1, Elsevier, Amsterdam.

DESAI, V.S. & FORBES, R.E. 1971 Environment and Geophysical Heat Transfer 4, 41.

DUMORE, J.M., MERK, H.J. & SPRINS, J.A. 1953 Nature 172, 460.

EDE, A.J. 1951 Proc. 8th Int. Cong. Refrigeration, 260.

ELDER, J.W. 1965 J. Fluid Mech. 23, 77.

FORBES, R.E. & COOPER, J.W. 1975 J. Heat Transfer 97, 47.

FUJII, T. 1974 Progress in Heat Transfer Engineering 3, 66.

GEBHART, B., BENDELL, M.S. & SHAUKATULLAR, H. 1979 Int. J. Heat Mass Transfer 22, 137.

GILPIN, R.R. 1975 Int. J. Heat Mass Transfer, 18, 13.

GRAY, D.D. & GIOGINI, A. 1976 Int. J. Heat Mass Transfer 19, 545.

LINTHORST, S.J.M., SCHINKEL, W.M.M. & HOOGENDOORN, G.J. 1980 ASME National Heat Transfer Conference, Orlando, HTD 8, 39.

MALLISON, G.D. & DE VAHL, Davis G. 1973 J. Comp. Phys. 12, 435.

MERK, H.J. 1954 Appl. Sci. Res. 4, 435.

MERKER, G.P., WASS, P. & GRIGULL 1979 Int. J. Heat Mass Transfer 22, 505.

MOORE, D.R. & WEISS, N.O. 1973 J. Fluid Mech. 61, 553.

OBORIN, L.A. 1967 J. Engng. Phys. 13, 429.

PATTERSON, J. & IMBERGER, J. 1980 J. Fluid Mech. 100, 65.

POOTS, G. 1958 J. Mech. Appl. Math. 11, 257.

QUACK, H. 1970 Wärmi-Und Stoffübertragung 3, 134.

ROACHE, R. 1976 Computational Fluid Dynamics, Hermose Publishers.

ROBILLARD, L. & VASSEUR, P. 1980 ASME National Heat Transfer Conference, Orlando, paper 80-HT-74.

SAITOH, T. & HIROSE, K. 1980 J. Heat Transfer 102, 261.

SCHECHTER, R.S. & ISBIN, H.S. 1958 A.I. Ch.E.J. Vol. 4 No 1, 81.

SEKI, N., FUKUSAKO, S. & SUGAWARA, M. 1977 Wärmi-Und Stoffübertragung 10, 269.

SCHENK, J. & SCHENKELS, F.A.M. 1968 Appl. Sci. Res. 19, 465.

TAKEUCHI, M. & CHENG, K.C. 1976 Wärmi-Und Stoffübertragung 9, 215.

TKACHEV, A.G. 1953 AEC - Tr - 3045, Translated from a publication of the State Power Press, Moscow - Leningrad.

VANIER, C.R. & TIEN, C. 1967 Chem. Eng. Sci. 22, 1747.

VANIER, C.R. & TIEN, C. 1968 Chem. Eng. Progr. Symposium Ser. No 82, 64, 240.

VERONIS, G. 1963 Astrophys. J., 137, 641.

VASSEUR, P. & ROBILLARD, L. 1980 Int. J. Heat Mass Transfer 23, 1195.

WATSON, A. 1972 Quart. Journ. Mech. and Applied Math. 15, 423.

WILKES, J.O. & CHURCHILL, S.W. 1966 A.I.Ch.E.J. 12, 161.

YEN, Y.C. & GALEA, F. 1969 Phys. Fluid 12, No 3, 509.

LIST OF FIGURES

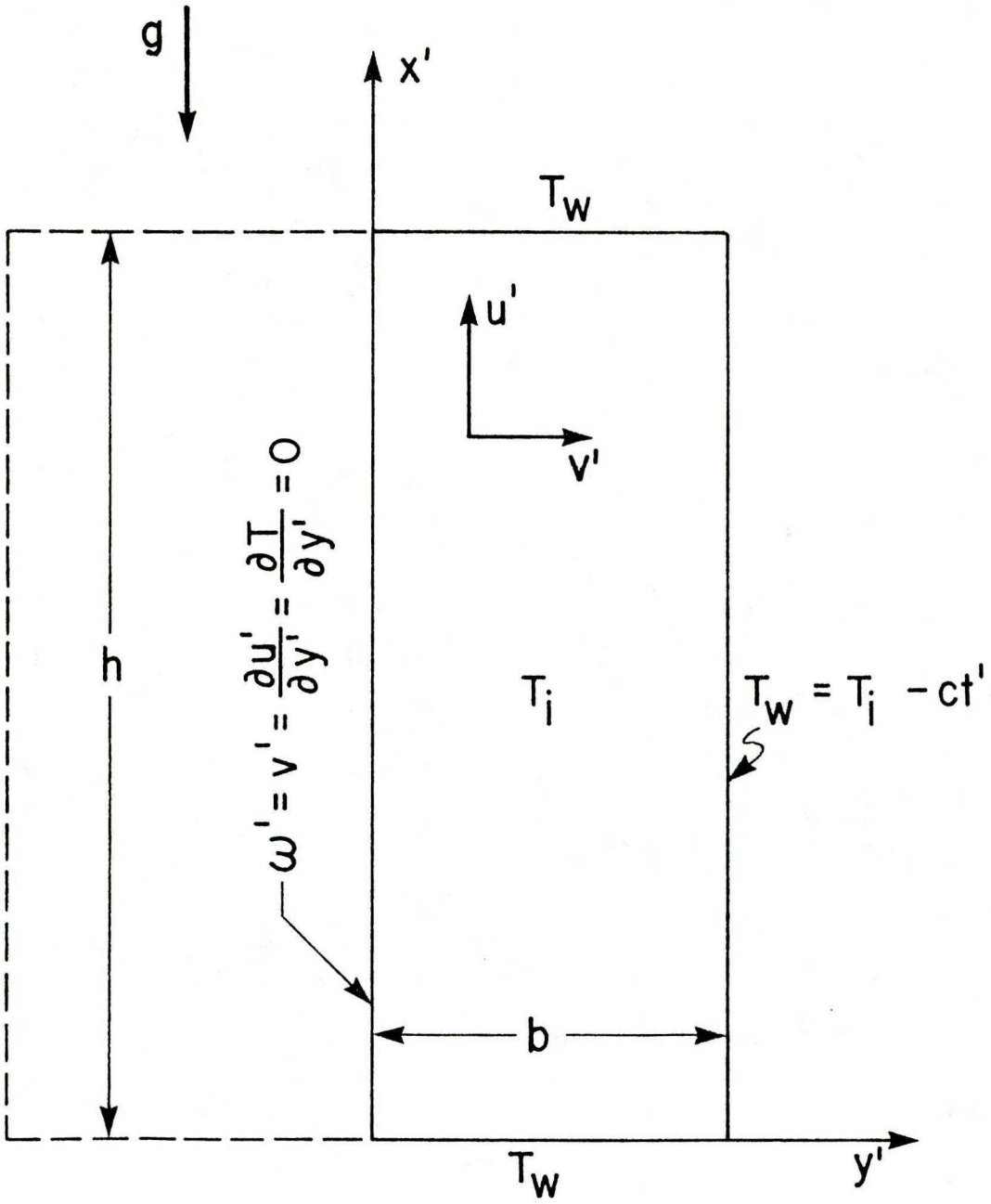

Fig. 1 Coordinate system and boundary conditions

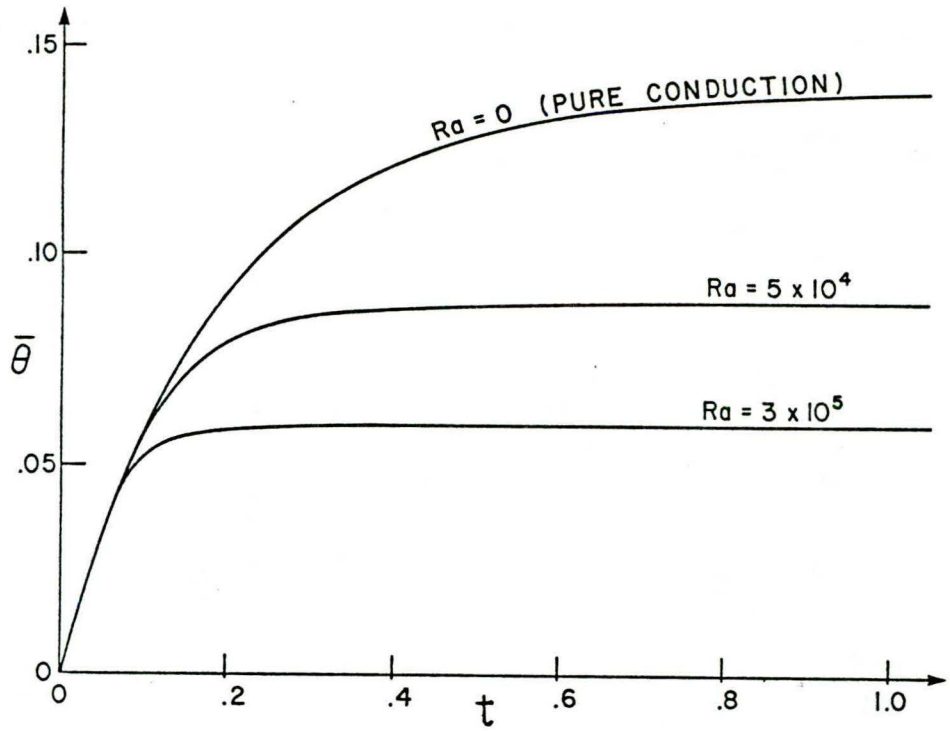

(a)

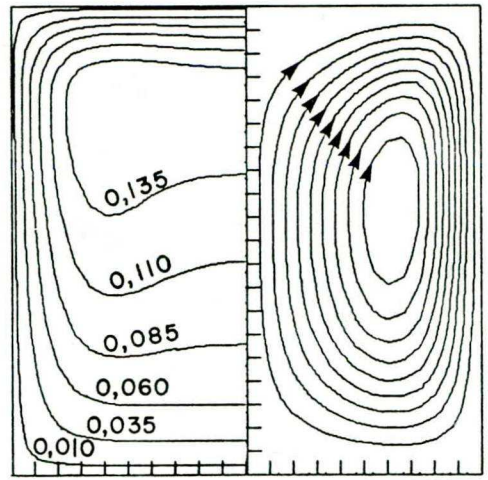

(b) Ra = 5 x 10^4

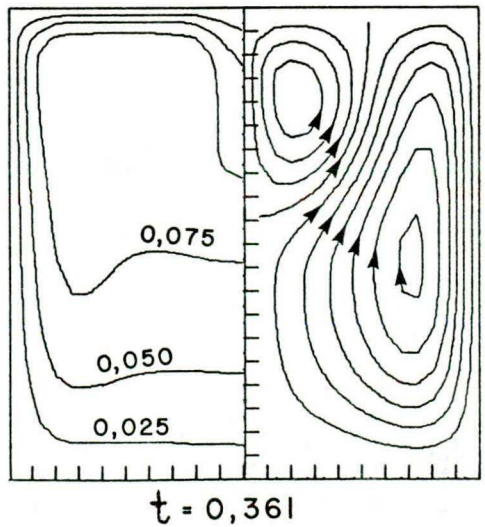

(c) Ra = 3 x 10^5

Fig. 2 Initial transients and quasi-steady state flow and temperature fields at constant Ra.

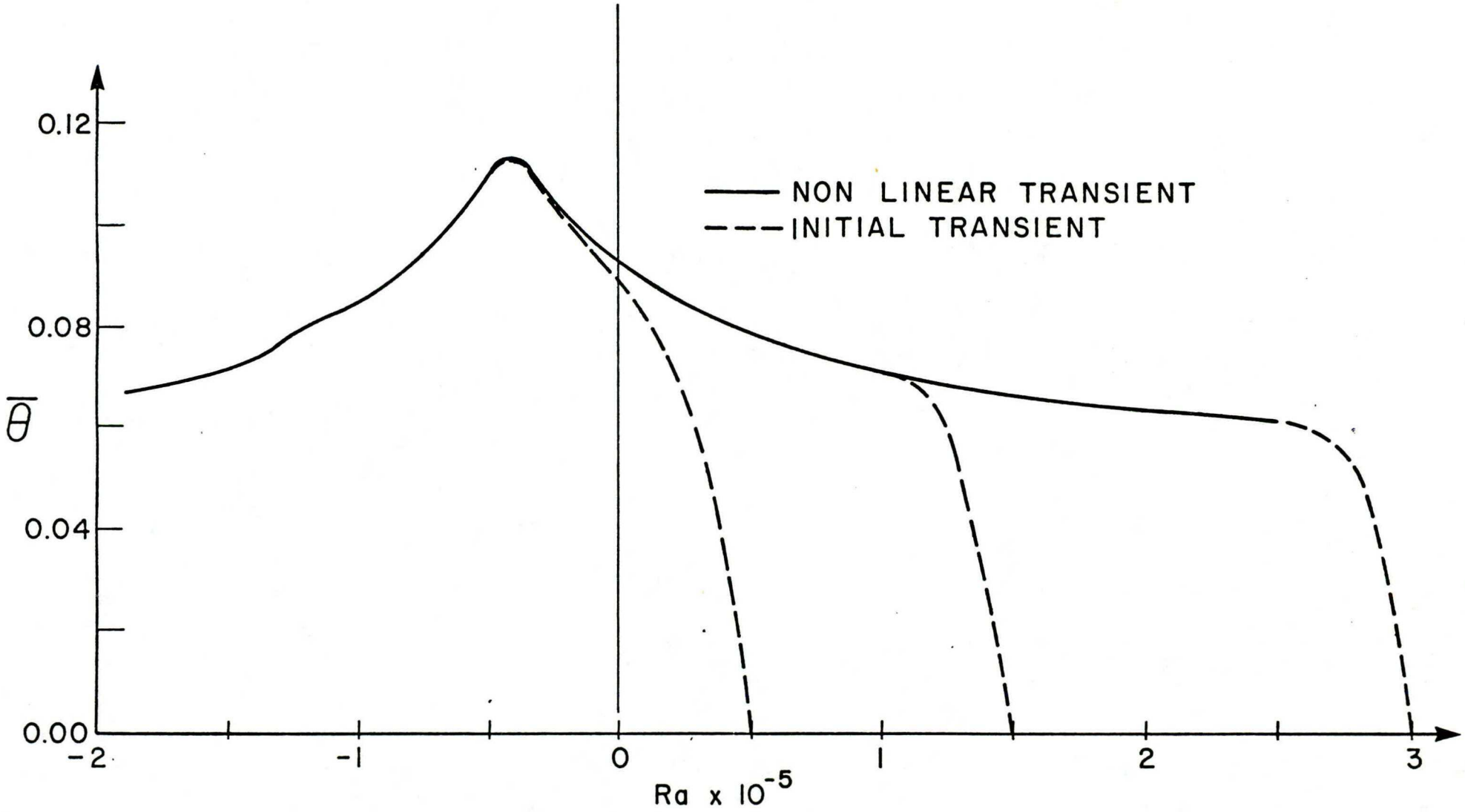

Fig. 3 Initial and non linear transients for Ra decreasing linearly with time (Ra' = 2 x 10^5)

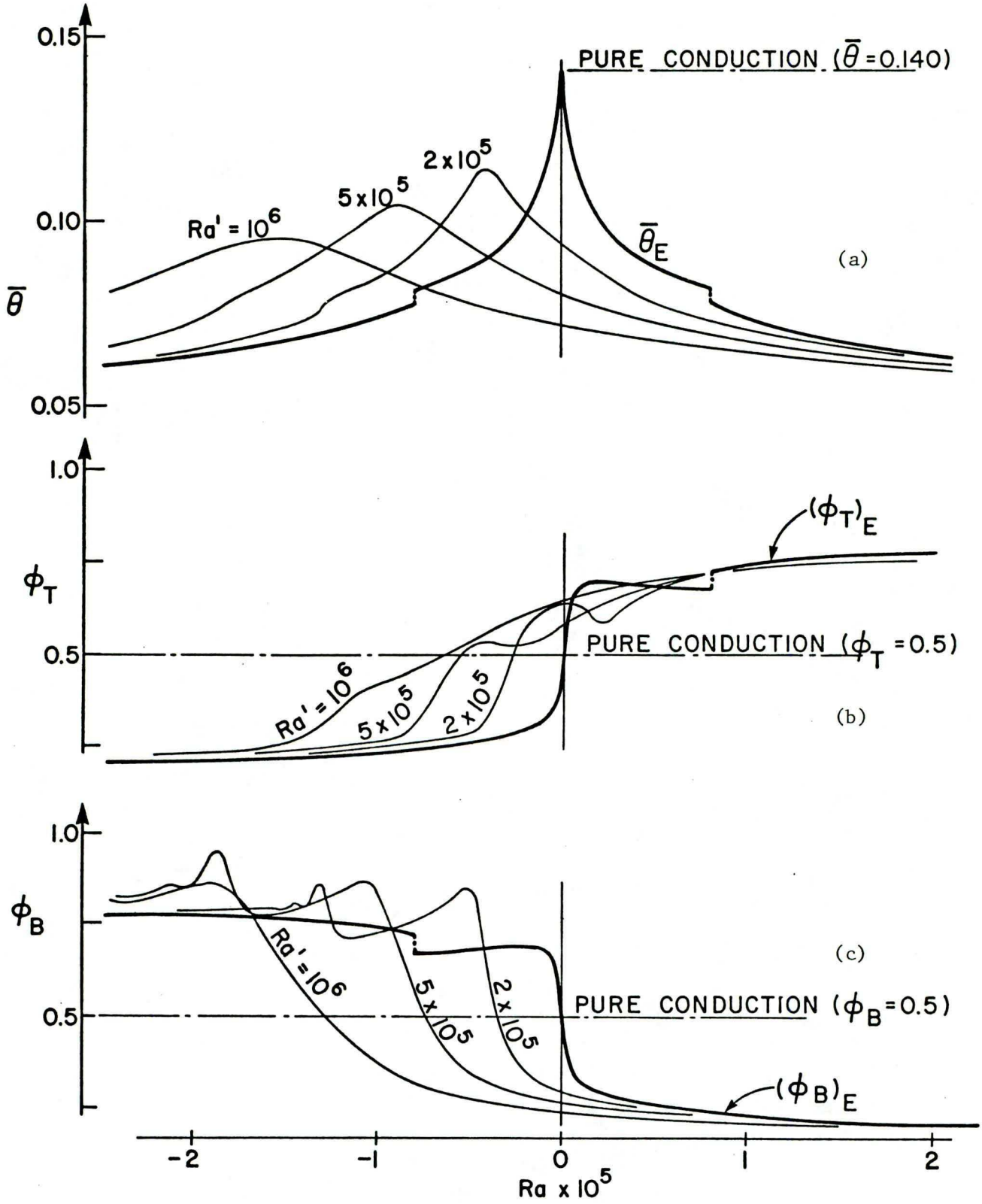

Fig. 4 Equilibrium state and non linear transients

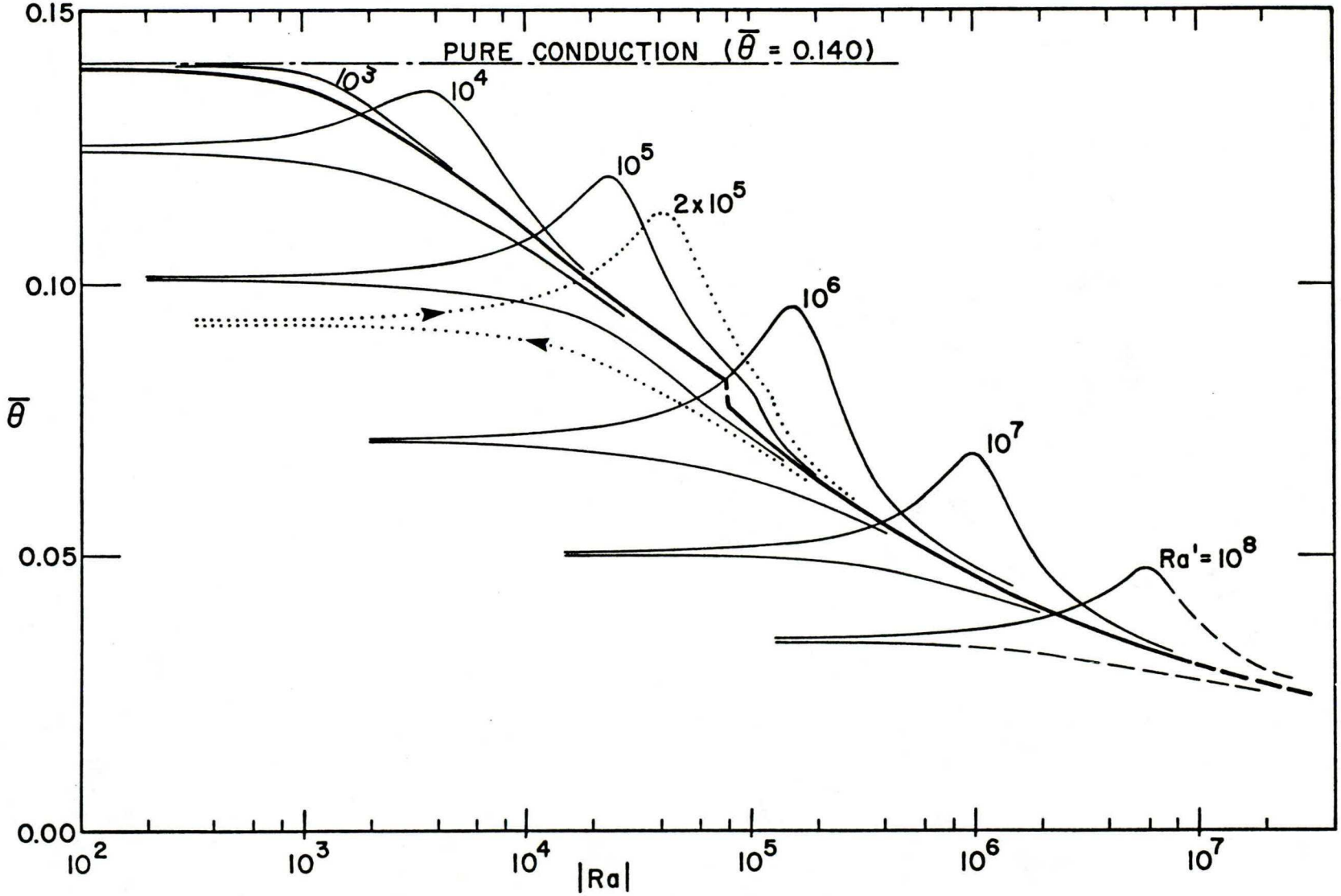

Fig. 5a Dimensionless temperature averaged over the cavity, function of Ra

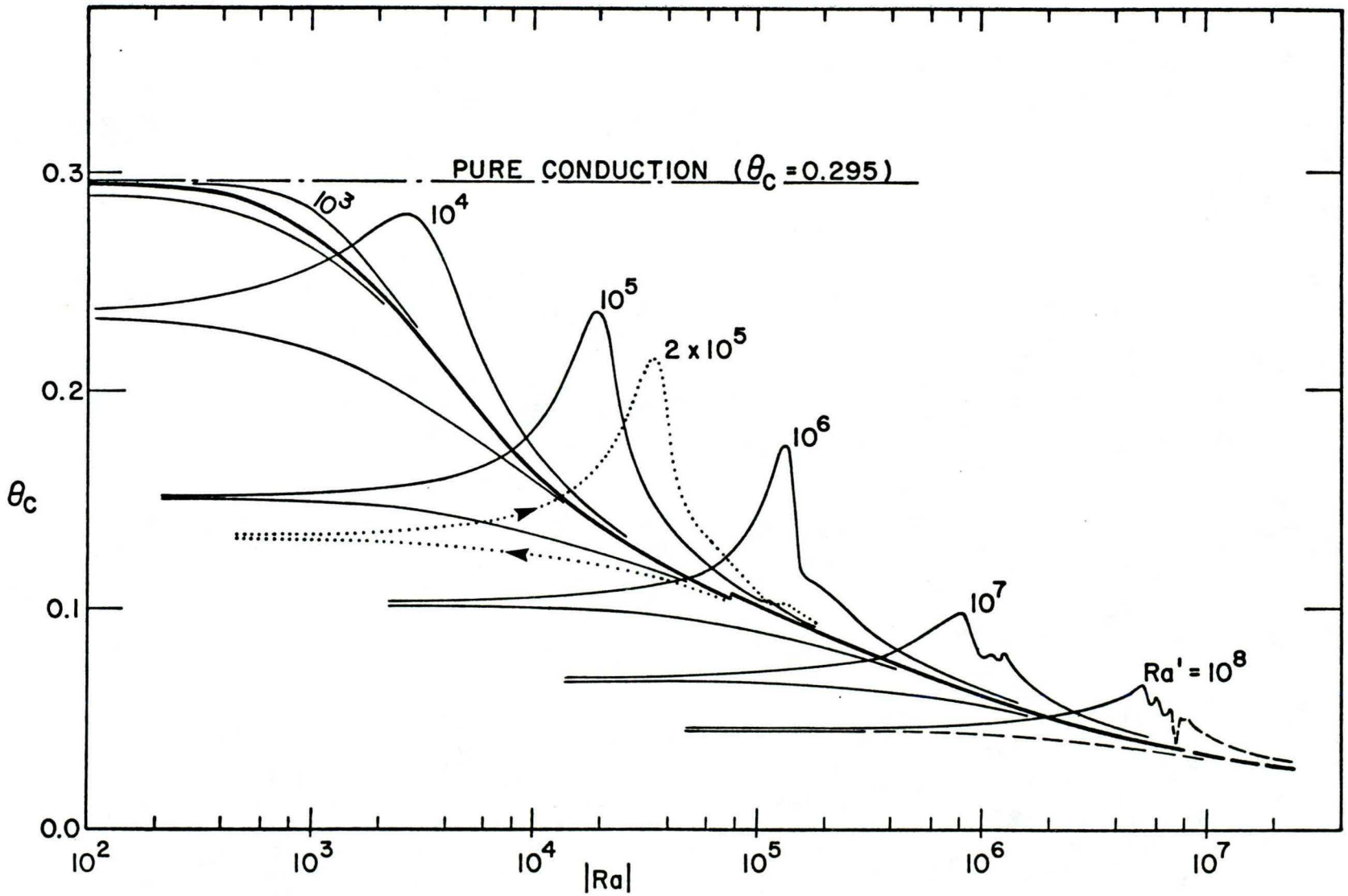

Fig. 5b Dimensionless temperature at the center of the cavity, function of Ra

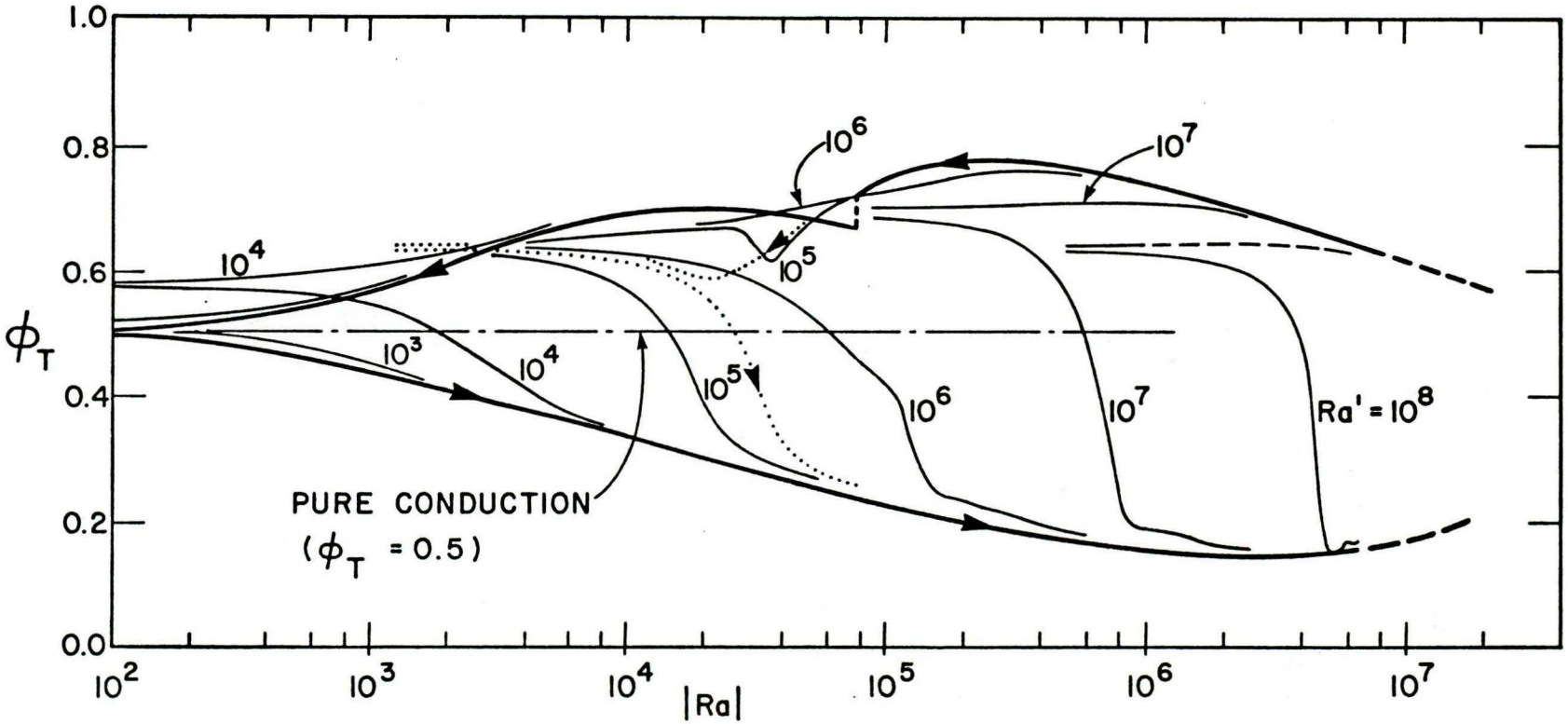

Fig. 5c Heat transfer at the top boundary, function of Ra

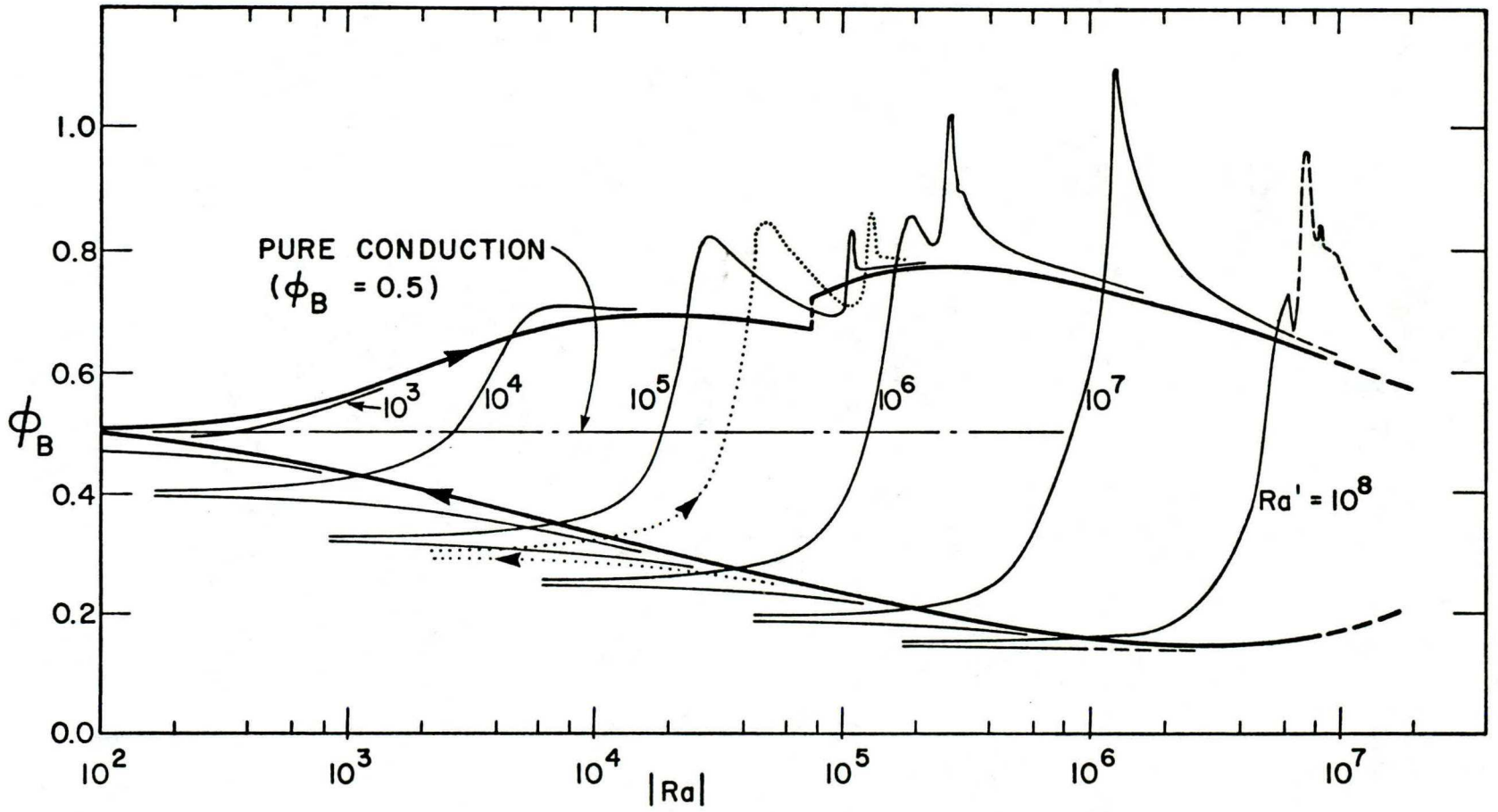

Fig. 5d Heat transfer at the bottom boundary, function of Ra

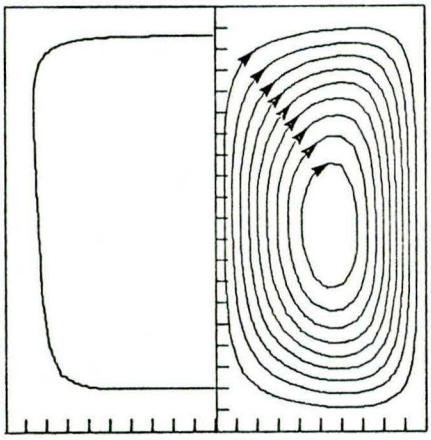

(a) $Ra = 1.40 \times 10^5$

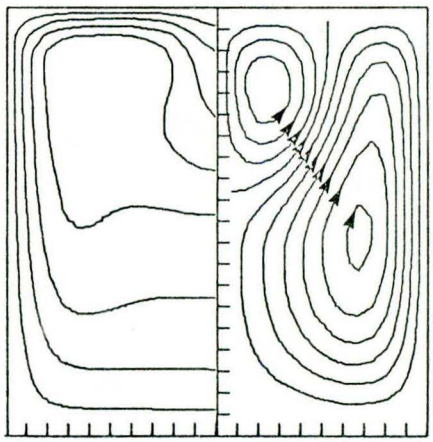

(b) 1.01×10^5

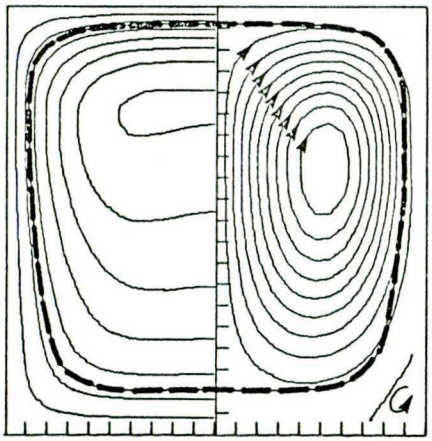

(c) -1.24×10^4

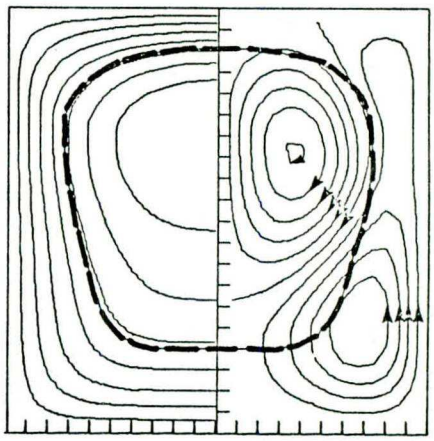

(d) -2.45×10^4

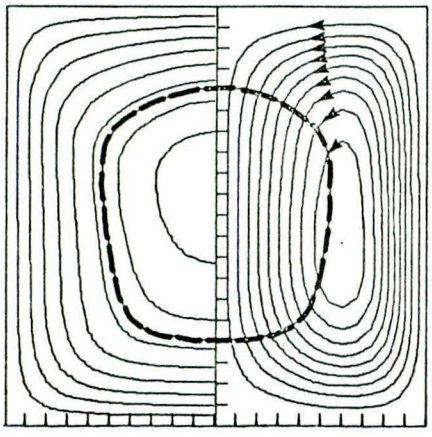

(e) -3.25×10^4

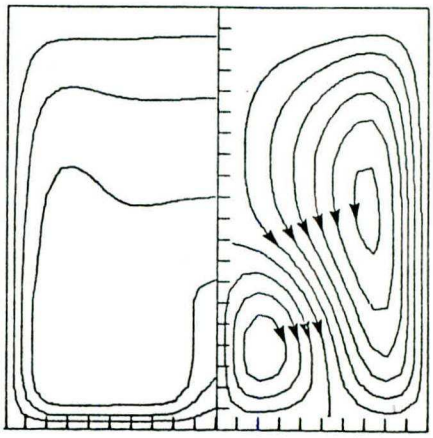

(f) -3.1×10^5

Fig. 6 Transient streamlines and isotherm field with $\Delta\theta = .025$, for $Ra' = 2 \times 10^5$ and $Ra_i = 1.47 \times 10^5$
(dashed line, where it appears, represent the 4°C isotherm)

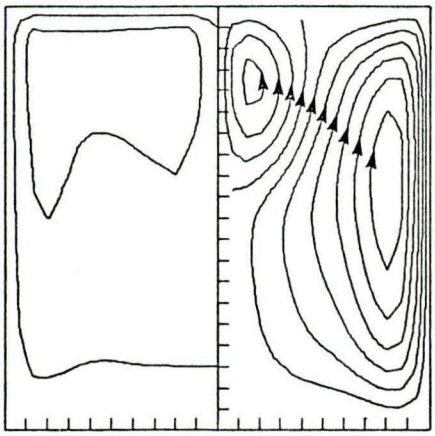

(a) Ra = 3.00×10^6

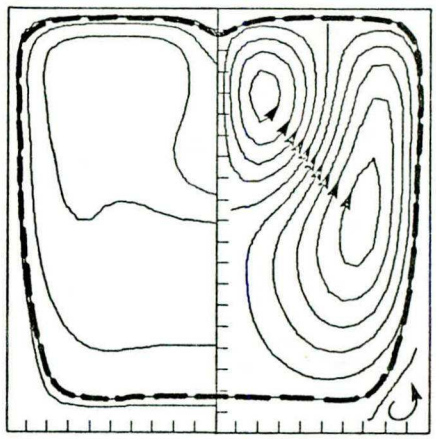

(b) -3.15×10^5

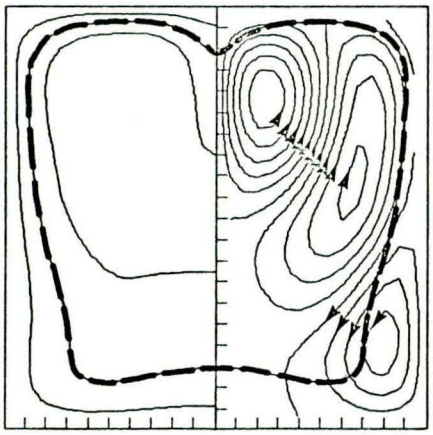

(c) -5.16×10^5

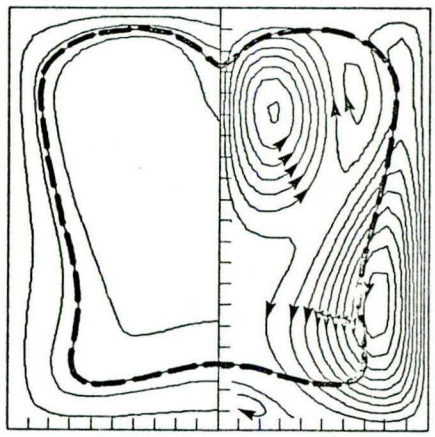

(d) -6.16×10^5

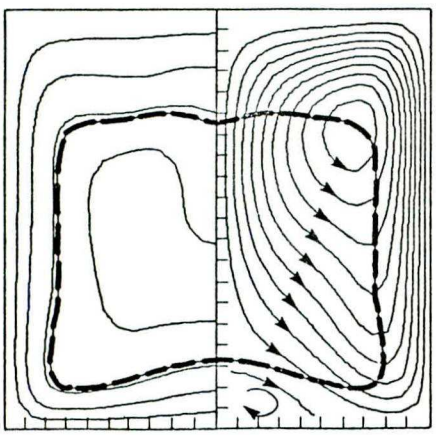

(e) -8.17×10^5

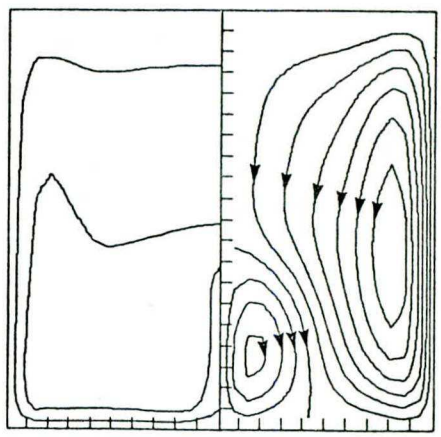

(f) -3.00×10^6

Fig. 7 Transient streamlines and isotherm field with $\Delta\theta = .025$, for Ra' = 10^7 (dashed line, where it appears, represents the 4°C isotherm)

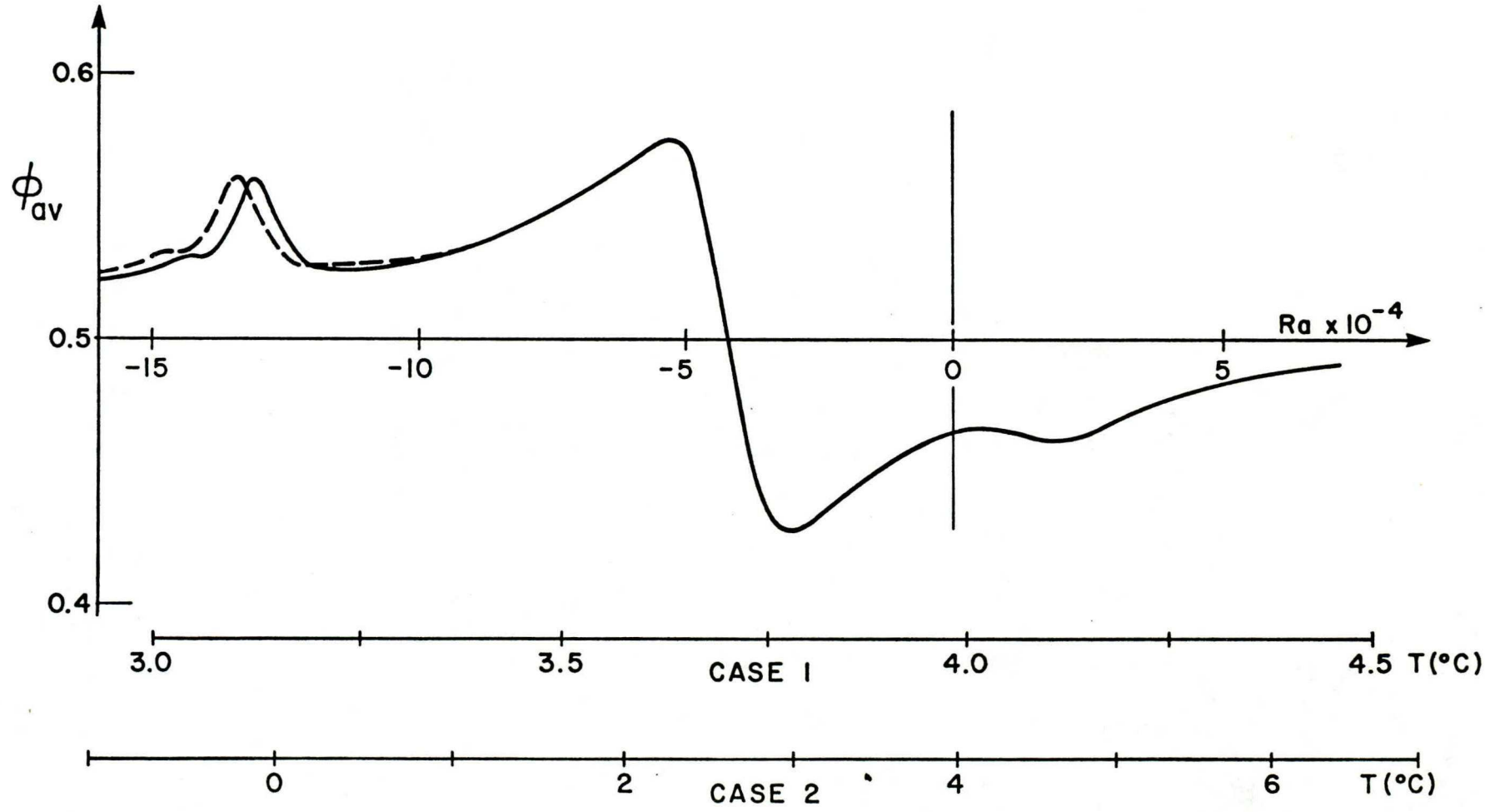

Fig. 8 Non linear effects of relationship between β and T (Ra' = 2 x 10^5)

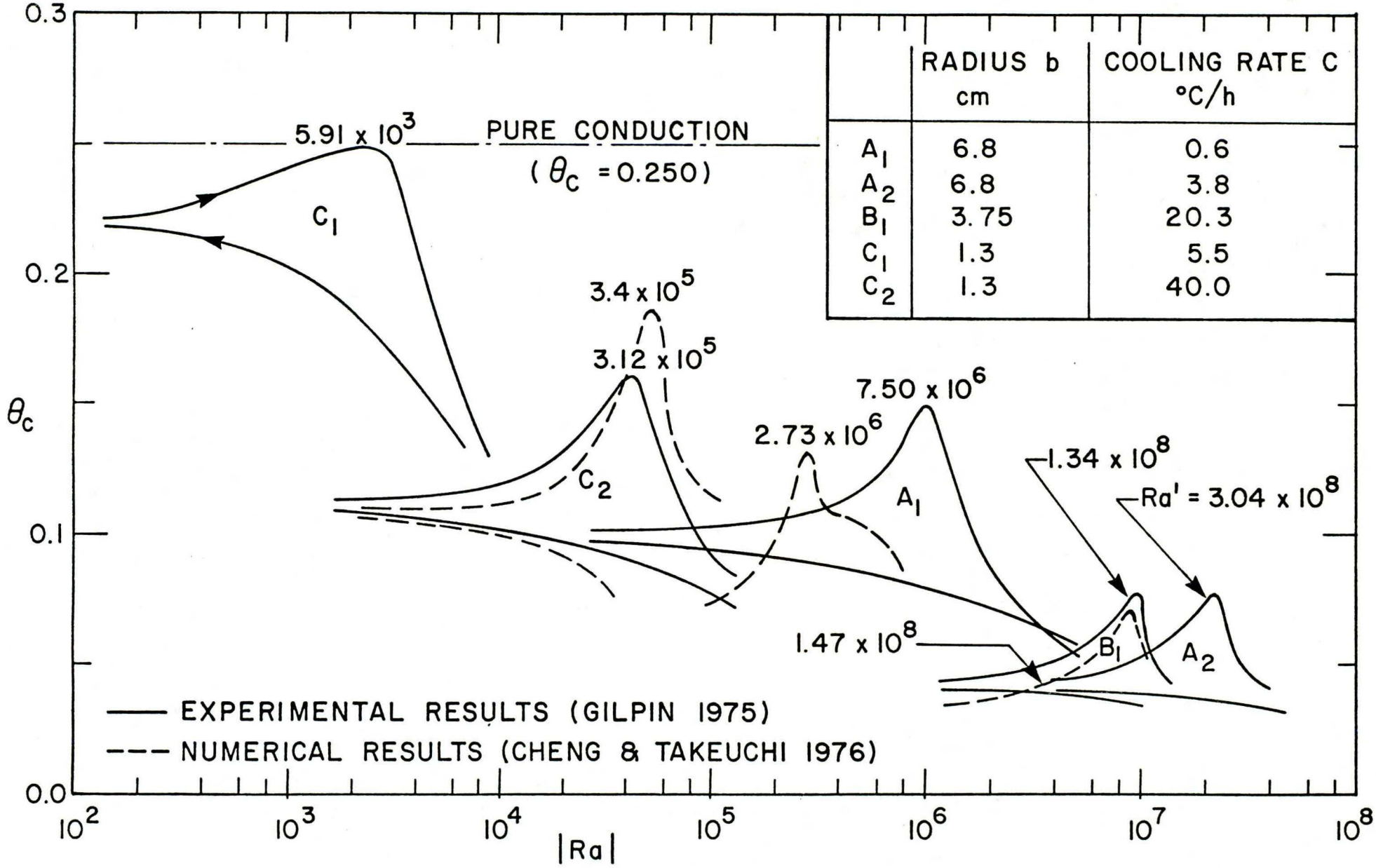

	RADIUS b cm	COOLING RATE C °C/h
A_1	6.8	0.6
A_2	6.8	3.8
B_1	3.75	20.3
C_1	1.3	5.5
C_2	1.3	40.0

Fig. 9 Horizontal circular cylinder filled with water and cooled at a constant rate.